# Guidelines for accurate current-voltage measurement of high-efficiency c-Si solar cells

Jacques Levrat, Jonas Geissbühler, Bertrand Paviet-Salomon, Christophe Ballif and Matthieu Despeisse, CSEM, Neuchâtel, Switzerland

## Abstract

The market for commercial crystalline silicon (c-Si) solar modules has been ruled for decades by the well-established ribbon-interconnected Al-BSF solar cells, making their metrology and in particular the current-voltage measurement well defined and reproducible. The recent appearance of high-efficiency technologies at mass production level, such as PERC, PERT, heterojunction or back-contacted, coupled to advanced module designs like multi-wire or shingle interconnection, sometimes in bifacial configuration has raised some metrological concerns. In most cases, no norms were in place, leaving manufacturers free to rate the power of their devices by a procedure of their choice. As the pricing of solar cells is based on their energy conversion efficiency in standard test conditions, such a situation is not suitable either for manufacturers or for customers. Indeed, without a well-defined framework for the measurement, the module manufacturer and of course, the final customer, might pay a wrong price. The present contribution aims at giving an overview of the new challenges that high-efficiency c-Si solar cells are facing when it comes to assessing their optical and electrical performances, as well as providing guidelines for their accurate measurement.

## Introduction: from Al-BSF design to high efficiency solar cells

The first diffused-junction silicon solar cell was developed by Pearson, Fuller and Chapin on n-type silicon in 1954 [1] and featured an energy conversion efficiency of 6%. It took then decades of development to master the mass production and achieve interesting efficiencies with the Al-BSF structure in the early 80s. This cell architecture has set the standard in industry for three decades but has now reached its physical limits, with up to 20.3 % efficiency demonstrated [2]. It represented about 90% of the global PV production in 2013 and down to 70% in 2017 with a decay expected to continue until this technology only marginally exists in about 10 years [3].

The main driver for this market change is the progressive upgrade of the production lines toward PERC cell designs that enable cell efficiencies well over 20% at competitive costs. In this respect, LONGi recently demonstrated record efficiencies of 23.6% on monofacial PERC [4]. In parallel, alternative Si-based technologies featuring higher conversion efficiencies combined with a more important room for improvement are appearing. The more important ones are silicon heterojunction (SHJ) and back-contacted (BC) solar cells encompassing interdigitated contacted (IBC) and metal wrap through (MWT) cell designs. Unlike the PERC design, IBC, MWT and SHJ designs cannot be manufactured on existing production lines as they involve different fabrication processes. For this reason, their aggregated market share does not exceed 5%, despite very high conversion efficiencies: 23.1% on SHJ MWT [5], 25.1% on both-side contacted SHJ [6] or 26.7% on SHJ IBC [7]. Note that these technologies are becoming more and more mature and cost-competitive and should significantly increase their market share in the coming years according to ITRPV annual report [3].

## New metrological challenges

High-efficiency solar cells have come with optical and electrical challenges for the measurement of their performances. In particular, bifaciality, higher intrinsic capacitance or new metallization/interconnection patterns have brought complexity and currently available cell testers are no longer able to assess the power accurately. Interestingly, even the guidelines framing the data processing of IV curves are no longer sufficient for devices featuring too high fill factors.

### Bifaciality

One of the most striking features is that all the above-mentioned cell designs (with the notable exception of Al-BSF) are intrinsically bifacial, i.e. their back metallization can be opened to enable light absorption from both sides. From a metrological point of view, this property raises serious questions such as: how to account for bifaciality? How to handle the parasitic optical feedback from the contacting unit? What can be reasonably measured in a production line? How to value the bifacial gain to the final customer? How to ensure standardized and comparable IV measurements?

These interrogations will soon be answered by the new IEC standard that defines the measurement procedure and requirements for bifacial cells and modules [8]. Unlike monofacial devices, IV measurement is performed on front and rear sides successively to extract the bifaciality coefficients. Optical feedback on the rear-side induced by the contacting unit should not exceed

3W/m$^2$, i.e. 0.3% of the incident power. To do so, two valid approaches are suggested:

- Use a rear-contact unit that fulfills the 3W/m$^2$ recommendation, typically a non-conductive and non-reflective material with local contacting areas.
- Use a set of rear-contact units featuring different reflectivities. Then, the intrinsic short-circuit current can be extracted with a linear regression [9].

Once the two sides are measured, the front- and rear-side parameters allow the extraction of the bifaciality parameters $\varphi$ for $I_{sc}$, $P_{max}$ and $V_{oc}$ according to the formula:

$$\varphi_X = \frac{X_r}{X_f} \quad (1)$$

Where X stands either for $I_{sc}$, $P_{max}$ or $V_{oc}$ and f and r, for the front and rear side configurations, respectively.

In a second phase, the bifacial gain is highlighted by flashing the device in field-equivalent conditions, where 10% to 20% of additional irradiance is collected from the surrounding albedo. To mimic these situations, the device is flashed at minimum three irradiances. Two approaches are suggested:

- ***The "$G_E$ – method" (or equivalent irradiance method)***
  To achieve an effective rear irradiance $G_r$ [W/m$^2$], the front side is flashed with an equivalent irradiance $G_E$ defined as:

$$G_E = 1000\left[W/m^2\right] + \varphi\, G_r \quad (2)$$

$G_r$ is usually comprised between 0 and 200 W/m$_2$ and $\varphi$=min ($\varphi\, I_{sc}$, $\varphi\, P_{max}$) is the device bifaciality.

- ***The dual illumination method***
  Here, the front light source flashes either at 1,000 W/m$^2$ (front side configuration) or at 0 W/m$^2$ (rear side configuration). For the higher irradiances, i.e. 1,000 + $G_r$ [W/m$^2$], the front light source flashes at 1,000 W/m$^2$ and the rear one at $G_r$ [W/m$^2$].

For the device labelling, the values of $P_{max}$ at STC with $G_r$ = 100 W/m$^2$ and $G_r$ = 200 W/m$^2$ must be indicated and are labelled $Pmax_{BiFi1o}$ and $Pmax_{BiFi2o}$, respectively.

Beside hardware differences, the two methods feature different injection profiles for the configurations at irradiances higher than one sun, as in the first approach the light is absorbed from the front side only. For the short-circuit current, one could expect than nonlinear cells might suffer from this anisotropic injection. However, a study from Fraunhofer has shown that such a nonlinearity has no detectable impact on $I_{sc}$ determination and the two approaches are fully equivalent [10].

Regarding the fill factor (FF), more discrepancies can be observed when comparing front and rear-side illuminations. If one considers low quality bifacial PERC solar cells, the situation might become noticeable. For light incident on the back surface field side (rear side), the carrier transport to the emitter side is driven by diffusion and leads to an important accumulation of charges at the interface and therefore to an enhanced recombination. For poor lateral conductivities or badly conductive fingers, $I_{sc}$ and FF might be affected. Conversely, for light incident on the emitter side (front side), carrier transport through the structure is driven by the internal electric field, making the carrier distribution more flat through the structure and fewer charges accumulate at interface [11]. This asymmetry is real and should be reported as such in the bifaciality coefficients, as recommended by the norm. The question that arises is the equivalence between the GE-method and the dual-side illumination at higher injections, i.e. the 1000 + $G_r$ case. No conclusive study has been conducted so far on cells (some are ongoing), but it is expected that the two methods are equivalent as the cell is already under "high" injection when the irradiance is increased from the 0 to 200 W/m$^2$ on the rear side.

In production lines, it might not be necessary to go through the full sequence that requires five flashes and eventually one cell flipping in case only one lamp is used. It would make sense to flash all cells in standard test conditions on the front side and use a non-reflective chuck or use dual-side flashing, taking great care that no parasitic light can hit the rear side of the cell, in agreement with IEC norm [8]. The information related to bifaciality, i.e. $\varphi$, $Pmax_{BiFi1o}$ and $Pmax_{BiFi2o}$, would be given on a statistical basis, as for the thermal coefficients. Keeping the number of flashes per cell at its minimum will maintain a high throughput and costs at a lower level.

## Advanced metallization

Contacting quality can be challenging for new cell technologies as they do not necessarily follow well-defined standards for metallic patterns. Metallization has become a fantastic playground for manufacturers to improve their cell efficiency and lower their costs: square cells with few busbars arranged in the so-called H-pattern is not anymore the only way to go. New patterns and cell configurations are appearing and calling for dedicated metrological solutions and standards. In the following, we list the recent trends in cells manufacturing.

## Back-contacted cells

An interesting approach towards high cell efficiencies is to decrease the optical losses occurring at the front of the device by placing all terminals on its rear side. For instance, IBC cells are completely metal-free on front side and feature a

dense comb-pattern alternating p and n polarities at the rear-side. MWT cells explore non-standard metallic geometries on front side optimized to reduce the optical and resistive losses. The generated current is then collected at the backside through metallic pads.

In both cases a careful attention must be paid to the bifaciality. Moreover, as n and p polarity terminals are located at the rear-side they cannot be measured with a conventional contacting units or bars. A dedicated contacting layout with distributed current and voltage probes must be set up. Among them, we can cite the two following approaches:

- ***The pin-based approach***
  This approach consists of using a non-conductive contacting unit where spring-loaded pins probing the voltage and the current are inserted. This approach is very convenient if the cell metallic design is fixed. In case of frequent variation of the metallic pattern, the rear contacting unit must be replaced each time.

- ***The PCB approach***
  If the rear side pattern of solar cells is frequently evolving over time, it is important that various metallic patterns can be measured without the need for expansive setup modification. This idea of flexibility at low costs is possible with the PCB approach, like the PCB$^{TOUCH}$ developed and patented by PASAN [12]. The base contacting system is always the same, only the PCB is replaced from one cell pattern to another.

## New patterns for advanced module designs

Beside back-contacted technologies, it is also very interesting to see how the module designs have dictated new rules for metallization. The most striking current applications are new interconnections like multi-busbars, multi-wires, shingles or cut cells [13].

## Multi-busbar and multi-wire

H-patterned Al-BSF cells with two or three busbars require a lot of costly metallic paste and induce important shadow losses. The trend today is to further increase the busbar number to four, five or six but with reduced widths. Narrower tabs and finger lines reduce the metal usage while decreasing the shadow losses and also improving the aesthetics of the module. The multi-busbar approach from SCHMID pushes this trend to an extreme by implementing 12 (or more) narrow "busbars", typically thinner than 0.5 mm [14]. IV measurements might become problematic due to the increased projected shadowing during the contacting. Such configuration might not be representative of the field application. CSEM is currently evaluating the impact of irradiance spatial inhomogeneity during IV measurement that could potentially affect FF and $V_{oc}$.

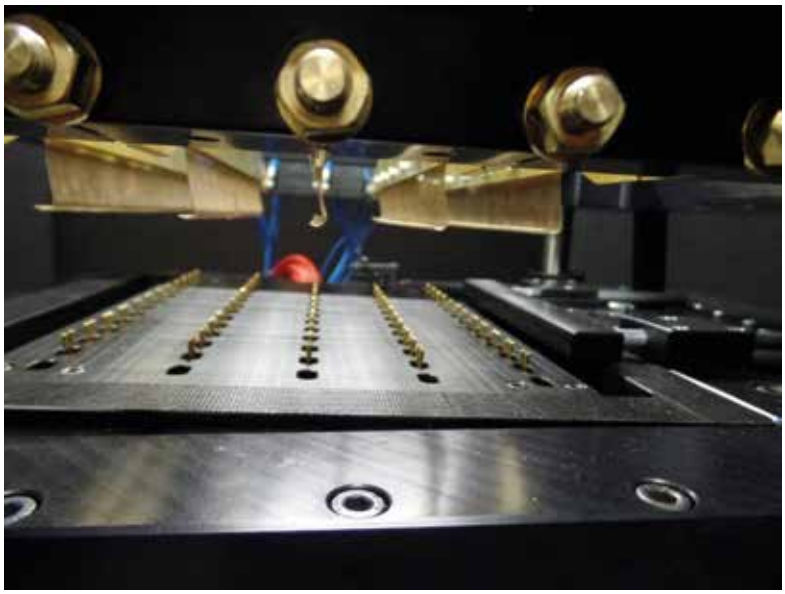

**Figure 1. h.a.l.m. contacting unit for busbarless solar cells.**

When further increasing the busbar number, it might no longer be cost-effective to print them. The multi-wire approach involves removing them completely. Instead they will be replaced by soldered interconnectors during lamination. This is achieved with the SmartWire Connection Technology (SWCT) [15]. When the number of extracting lines N increases, the finger losses decrease as $1/N^2$ and become completely negligible when N > 15 or 20 (depending on the line resistivity). As the finger electrical losses no longer impact the FF, ultra-fine lines can be printed which considerably lowers the silver usage and costs but also decreases the shading. From a metrological point of view, ensuring a 100% rate of contact on such shallow lines is a real challenge. Nowadays, two competitive approaches are available:

### *Approach 1: Finger contacting with hooks*

This solution (see Fig. 1) has been developed by h.a.l.m. and consists in five contacting bars, each of them containing one metallic hook per finger. This approach ensures a one-to-one contact and a good measurement reproducibility [16].

### *Approach 2: Finger contacting with wires*

The so-called Grid$^{TOUCH}$ (see Fig. 2) developed and patented by PASAN [17] from the Meyer Burger group (that developed the SWCT technology) consists of 30 wires for current extraction and five wires for voltage measurement [18]. The rear contacting is either ensured by wires with the same configuration or by a PCB. A slightly bent plateau ensures a homogeneous contact. The certification institute CalLab (Fraunhofer ISE) is following this approach.

Once the busbars have been removed and replaced by interconnecting wires at the module level, the cell-to-module (CTM) loss analysis is no longer defined for the grid losses. The reason is very simple: grid losses depend on the mean distance travelled by electrons through the metallic grid. For

busbarless cells, this value is fixed at the module level only. As the cell measurement geometry does not necessarily correspond to the extraction geometry at the module level, IV cell parameters must be corrected to allow a one-to-one comparison between cell and module, like for standard cells where the busbar number equals the ribbons number.

In the first approach, only five arrays of hooks are present and in the second approach, 30 wires serve the same goals. Typically, the number of wires in the module is close to 15 depending on their diameter. It is clear that both methods are not giving FF corresponding to the final application. Figure 3 shows how the grid losses will contribute to the device losses depending on the number of bars or wires used for current extraction. Clearly, for a standard busbarless module design containing 15 to 20 wires, the approach with hooks (five measuring bars) underestimates the FF, whereas the wire approach (30 measuring wires) overestimates it.

Beside the electrical mismatch between cell and modules, busbarless cells are measured without the impact of shadowing as the irradiance is adjusted to compensate the contacting unit shadowing. Whereas this effect is fully accounted for in the CTM analysis of standard cell with busbars, the IV cell parameters must be corrected to account for the presence of interconnectors. Otherwise the cell efficiency would be artificially too high and no fair comparison could be made with identical cells featuring a standard print with busbars.

Correcting the electrical and optical losses does not impact in any way the final module power but only the attribution of losses between cell and module. The CTM analysis will in the end contain the exact same terms but some of the module losses are transferred to the cell ones via the effective efficiency approach that sets busbarless and standard cells on equal footing. The corrections requires the following inputs:

- ***Optical correction:*** Cell size L, wire number Nw and diameter Dw
- ***Electrical correction:*** Grid resistance of front and rear sides, GRf and GRr [Ohm/cm], respectively

The effective IV key parameters are given by the following set of equations [19]:

$$I_{sc,eff} = I_{sc,meas}(1 - s) \tag{3}$$

$$I_{mpp,eff} = I_{mpp,meas}(1 - s) \tag{4}$$

Where $s \approx \frac{N_w D_w}{L}$ is the shadowing due to interconnectors in the final module. To apply this

$$V_{oc,eff} = V_{oc,meas} + \frac{kT}{I_{sc,eff} q} ln(1 - s), \quad for\ s < 5\% \tag{5}$$

$$V_{mpp,eff} = V_{mpp,meas} + \frac{kT}{q} ln(1 - s) - \frac{L}{12 N_w^2}\left(GR_f + GR_r\right) I_{mpp,meas} \tag{6}$$

approach, the cell tester manufacturer must also provide a grid resistance diagnostic, which is the case for the products of two previously mentioned companies: h.a.l.m. and PASAN.

### Cut cells and shingles

The module industry is also innovating by modifying the cell shape with the goal of achieving higher efficiency by increasing the voltage and decreasing the current. Doing so, the resistive losses are reduced but optical gains are also expected [13]. One approach is to dice the cells parallel to the fingers into halves or quarters. With this approach, the interconnection strategy is unaltered as well as the cell contacting. The second popular approach is to cut the cells perpendicularly to fingers along the busbars. Cell interconnection is trickier as it no longer involves metallic contacts: the cells are stacked on top of each other with electrically conductive adhesives. These so-called "shingles" would be more challenging to measure, in particular if made bifacial, as a single busbar would lie along the cell border. In practice, these cells are measured on the full wafer, prior to laser cutting for economic reasons: segmenting the cells in N parts would decrease the throughput by the same factor.

## Capacitive effects

Solar cell capacitance has two main origins: the junction capacitance Cj in the depletion layer and the diffusion capacitance Cdiff. For an abrupt junction, the former term reads [20]:

$$C_j = A\sqrt{\frac{q\varepsilon_s}{2(V_{bi}-V)}\left(\frac{N_A N_D}{N_A+N_D}\right)} \quad (7)$$

Where A is the cell area, q is the elementary charge, $\varepsilon$ is the semiconductor permittivity, $V_{bi}$ is the built-in potential, $V$ is the voltage applied to the capacitor, $N_A$ and $N_D$ are the acceptor and donor impurity concentrations. This term represents the accumulation of charges in the depletion layer and dominates the cell capacitance in reverse and low bias conditions. Under forward bias, the charge distribution of minority charge carriers in the bulk of the cell increases exponentially with the applied bias voltage. This charge is compensated by an equal distribution of excess majority carries at the other side of the junction. The associated capacitance reads [21]:

$$C_{diff} = C_0 e^{b\frac{q}{kT}V} \quad (8)$$

Where b is a fitting parameter, k is the Boltzmann constant and Co is the base capacitance given in the wide base diode limit by:

$$C_0 = \frac{q}{kT}\frac{qn_i^2}{N_A}L_n = \frac{q}{kT}\tau I_0 \quad (9)$$

$L^n$ is the base diffusion length, $\tau$ is the minority carrier lifetime and $I_o$ is the diode saturation current. In reality the exponential term is no longer valid above the maximum power point (MPP) because of interface states and another relation should be used to account for the Gaussian decrease of the capacitance [20]. Looking at equation 9, it is clear that technologies featuring low lifetime, and low base doping, will suffer less from capacitive effects. It is thus not surprising that Al-BSF cells are not limited by capacitive measurement artefacts, PERC only weakly and n-PERT more severely [22]. The situation gets even worse for IBC and HJT devices [Virtuani2012].

In case the sweep goes from short circuit (SC) to open circuit (OC) during the IV measurement, the carrier concentration raises, leading to an underestimation of FF and $V_{oc}$. Conversely, if the sweep goes from OC to SC conditions, the carrier concentration has to be lowered, leading to an overestimation of FF and VOC. [22]. The magnitude

**Figure 2. Grid$^{TOUCH}$, PASAN's contacting unit for busbarless solar cell.**

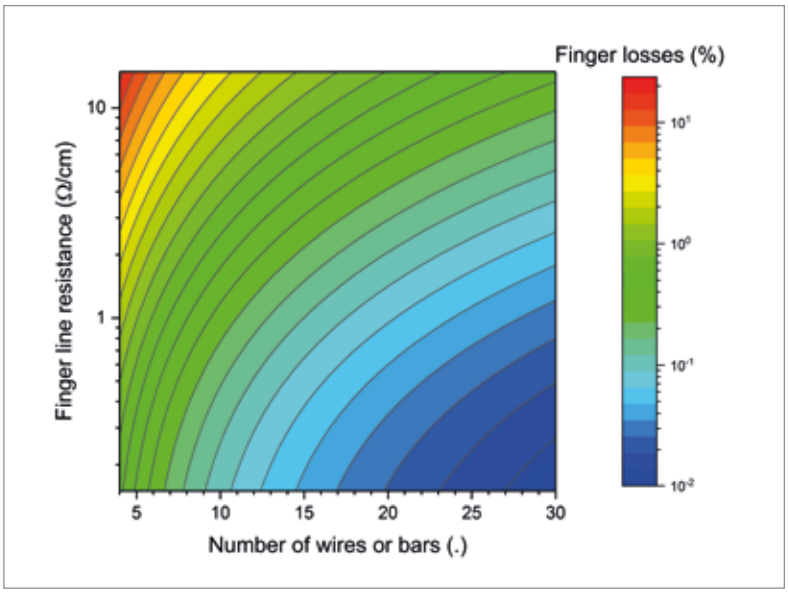


**Figure 3. Contribution of grid losses depending on the finger line resistance and on the number of contacting bars or wires.**

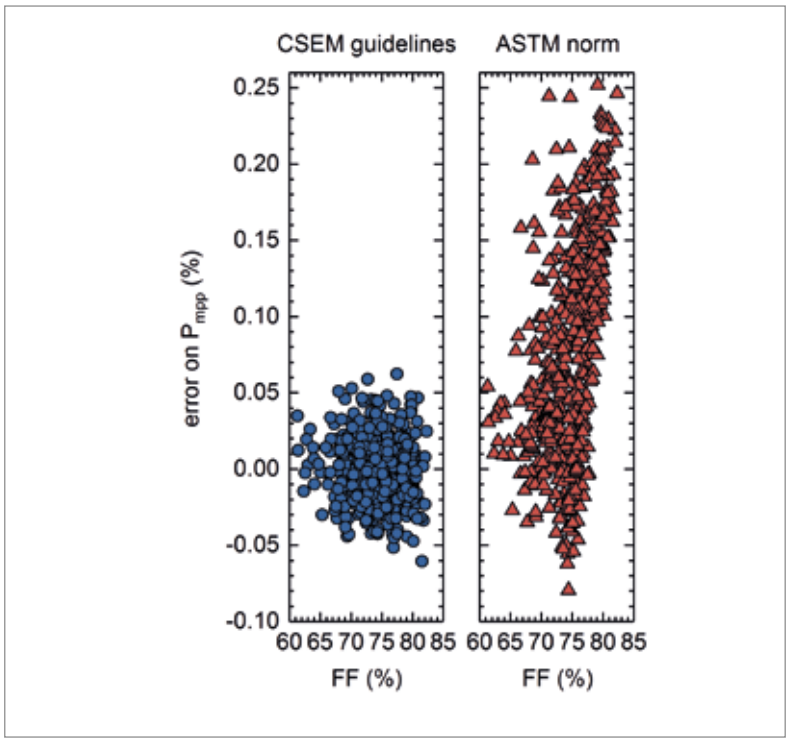


**Figure 4. Comparison of the error on Pmpp as a function of the FF of the device under test when applying the ASTM norm (right) and the CSEM guidelines (left).**

of the measurement error mainly depends on two parameters: the cell capacitance and the sweeping time. The shorter the sweeping time, the higher the cell capacitance, the higher is the measurement error. On the other side, the measurement time must be kept as short as possible to prevent undesired errors induced by radiation heating of the device. For this reason, the IV measurement must be carefully designed for high efficiency solar cells. Multiple approaches exist:

- ***Multi-flash***
  Increase of measurement time by flashing the device multiple times over segmented voltage ranges and reconstruct the IV curve in post-processing. Such approach can be very time-consuming and is not suited for the high throughput of industry.
- ***Optimized voltage ramp***
  Optimization of voltage ramp by slowing down acquisition time around MPP condition (or where the cell capacitance is limiting the cell response time). Such an approach allows flashing very capacitive solar cells with times compatible with industry standards.
- ***Photo and Dark Analysis (PDA) technology***
  The PDA method developed by KOPEL [23] is based on a comparison between a 50ms light-IV and a three-step sequence of dark-IV curves. The method assumes that light and dark IV have the same response with the exception of the series resistance contribution. The impact of cell capacitance is removed by calculating the internal cell resistance. The full measurement sequence does not cause any important heating of the device but requires an important measurement time for high capacitance devices.
- ***Hysteresis measurements***
  Hysteresis-based approaches rely on the fast sweeping of IV curves in forward and reverse biases. The resulting IV curves feature exotic shape because of the parasitic contribution of the voltage dependent cell capacitance. Nevertheless, these curves can be used to extract the cell capacitance and the true IV curves can be calculated with a proprietary algorithm based on an equivalent circuit. H.a.l.m. has implemented this approach on its cell tester to measure cells with high capacitance [24]. The main advantage is that the measurement is very fast and suited for the high throughputs of the industry but the generated IV curves are calculated from the measured ones and rely modelling.
- ***DragonBack***
  The 'DragonBack' technology has been developed by PASAN together with SUPSI [25]. It applies voltages above the set-point for each point on the IV-curve to accelerate capacitance loading. Then the voltage is reduced to the set-point value and kept stable until the current becomes stable. Fewer points are measured in the final IV curves, typically 15 to 20 but this has no impact on the accuracy of IV key parameters, i.e. $I_{sc}$, Voc and Pmpp, provided the voltages of these data points are carefully chosen [26].
- ***Voltage modulation***
  In this approach patented by Sinton Instruments [27], the voltage at the cell terminals is modulated by a small signal correction in order to suppress the measurement artifact produced by the cell capacitance.

## Data processing

In addition to several practical details known to alter the accuracy of IV curves measurements (most prominently fluctuations of the spectrum and the irradiance of the light source), the methods and the algorithms used to extract Pmpp from a given IV curve have been shown to lead in themselves to errors up to 2-3% [28, 29, 30]. To date, the ASTM E948-09 standard [31] is the only international norm specifically providing guidelines for Pmpp extraction. However, neither an estimation of the residual error on Pmpp, nor suggestions on how to adapt these guidelines to the performances of the device under test are provided. Based on numerically generated IV curves, we demonstrated that for devices with FF >75 %, the ASTM norm clearly overestimates Pmpp due to an inappropriate fit range, with errors as high as 0.25% (see Fig. 4 and Fig. 5). In contrast, adjusting the fit boundaries to the FF of the device under test eventually results in a three to fourfold reduction of the Pmpp error. Importantly, our new guidelines apply equally well on high and low density IV curves. Further details can be found in [26] and [32].

## Improved UV and infrared response and new light sources

The market of cell testers relies on well-established norms and standards. The light sources used to assess the performance of solar cells feature collimated light and continuous spectra, usually produced by Xenon flashes. As high-efficiency solar cells come along with higher capacitances, it is clear that the flash duration has become an important parameter that can be hardly tuned with Xenon tubes. For this reason, LEDs have recently attracted a lot of attention due to their high versatility in term of light pulse duration, irradiance control and spectral availability. The other important advantage of LEDs is their low maintenance costs, as they are relatively cheap and offer very long lifetime. The price of LEDs is however strongly dependent on their wavelength as different materials are involved: from blue to red they are really inexpensive but the situation changes for the near UV (<400 nm) and near-infrared ranges (>900nm) where availability, price and radiative efficiencies become limiting. However, the prices are going down and it is nowadays possible to achieve A+ spectra (according to the IEC60904-9:2007) at competitive costs. The availability and the prices of infrared LEDs is of paramount importance in the case of high-efficiency solar cells as they all feature improved quantum efficiencies in these spectral ranges: probing the UV ranges allows to probe surface recombination and parasitic absorption in the front layers whereas probing in the infrared gives an insight into rear surface recombination and light trapping efficiency. At the moment of the writing, many LED-based light sources are available for modules (MBJ, PASAN, Wavelabs, ECOPROGETTI, J. v. G. Thomas, Gsolar Power etc.) and cell testers (Wavelabs, Gsolar Power etc.). Alternative concepts are also emerging and combine the benefits of LED and conventional light sources. For example, PASAN SpotLIGHT is using a Xenon lamp for the $I_{sc}$ measurement and the calibration of red LEDs which are used during the voltage sweep. Alfartec is using a hybrid concept mixing LEDs and Halogen lamps to extend the spectral range in the infrared. More developments are expected in a near future that will enable cost reduction and a better compatibility with high efficiency solar cells.

## Conclusion

The prime goal of solar cell testers is to accurately assess the power of solar cells. For this reason, their architecture and mode of functioning must be constantly challenged, upgraded and validated. With the recent evolution of new solar cell designs at the commercial level, the needs for accuracy in the current-voltage measurement has become critical. The current lack of norms and directives framing the power rating of photovoltaic devices is problematic and the community has to rely on good practices and guidelines but also on reliable hardware compatible with all cell designs. The potential uptake of alternative technologies such as perovskite or perovskite-silicon tandem cells will very likely come with new requirements and problems. The validity of the measurement must therefore constantly be questioned, even in the (provisory) absence of metrological standards.

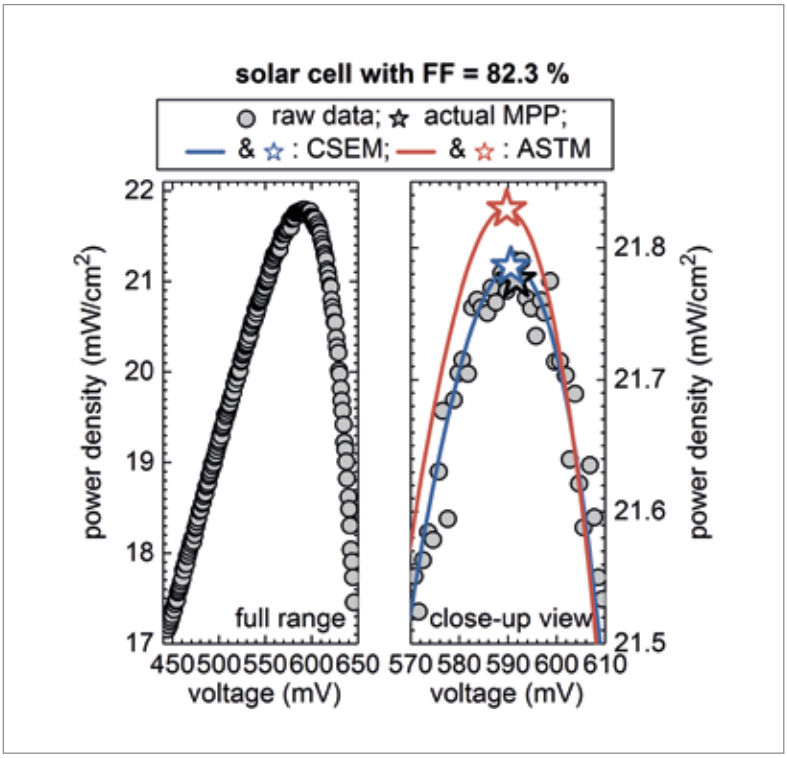


**Figure 5. Illustrative example of a solar cell with a high FF. The close-up of the MPP region clearly reveals that the ASTM norm leads to an overestimated Pmpp, whereas the CSEM guidelines prove much closer to the actual MPP.**

### References

[1] DM Chapin et al. 1954, "A new silicon p-n junction photocell for converting solar radiation into electrical power", *Journal of Applied Physics* 8, 676.
[2] Ki Hyung Kim et al. 2017, "Record high efficiency of screen-printed silicon aluminum back surface field solar cell: 20.29%", *Jpn. J. Appl. Phys.* 56 08MB25.
[3] ITRPV report, http://itrpv.net/Reports/Downloads/
[4] Press release by LONGi, "LONGi hits record 23.6% conversion efficiency for mono PERC solar cells", 28 February 2018.
[5] Press release by Japanese solar-PV manufacturer Choshu and Dutch energy research institute ECN, "New world record efficiency for large area metal wrap through silicon heterojunction solar cells", 15 June, 2016.
[6] D. Adachi et al. 2015, "Impact of carrier recombination on fill factor for large area heterojunction crystalline silicon solar cell with 25.1% efficiency", *Appl. Phys. Lett.* 107, 233506 (2015).
[7] K. Yoshikawa et al. 2017, "Silicon heterojunction

solar cell with interdigitated back contacts for a photoconversion efficiency over 26%", *Nat Energy*. 2(5):17032.
[8] IEC 60904: Photovoltaic devices, Part 1-2: Measurement of current-voltage characteristics of bifacial photovoltaic (PV) devices (in its approval phase at the time of writing).
[9] J. Hohl-Ebinger, W. Warta. 2010, "Bifacial Solar Cells in STC Measurement", *Proc. 25th EU-PVSEC*, Valencia.
[10] M. Rauer et al. 2017, "Bifacial Solar Cells und Single- and Double-Sided Illumination: Effect of Non-Linearity in Short-Circuit Current", *4th bifi workshop*, Konstanz.
[11] Ingrid Romijn 2017, "Bifacial solar cells - a brief overview", *4th bifi workshop*, Konstanz.
[12] J. Rochat, J. Hiller, N. Rebeaud, A. Ambühl. 2017, "Testing device", *Patent EP3126859*.
[13] R. Witteck et al. 2016, "Optimized Interconnection of Passivated Emitter and Rear Cells by Experimentally Verified Modeling", *IEEE Journal of Photovoltaics* 6, 432-439.
[14] J. Walter et al. 2014, "Multi-wire interconnection of busbar-free solar cells", *Energy Procedia* 55, 380 – 388.
[15] T. Söderström et al. 2013, "SmartWire Connection Technology" *Proc. of the 28th EU-PVSEC*, 495-499.
[16] S. Dauwe et al. 2017, "Precise IV-measurement of busbarless solar cells including process control methods for production", *6th Workshop on Metallization & Interconnection for Crystalline Silicon Solar Cells*, Konstanz.
[17] D. Bätzner, C. Clerc, E. Neto, P. Volluz, P. Beljean, B. Albers, P. Papet. 2015, "Testing device", *Patent EP2875366*.
[18] N. Bassi et al. 2014, "Grid$^{TOUCH}$: Innovative Solution for Accurate IV Measurement of Busbarless Cells in Production and Laboratory Environments", *29th EU PVSEC*, 1180 - 1185 (2014).
[19] P. Papet et al. 2017, Effective Efficiency of Busbarless solar cells", *6th Workshop on Metallization & Interconnection for Crystalline Silicon Solar Cells*, Konstanz.
[20] C. Monokroussos et al. 2006, "The Effects of Solar Cell Capacitance on Calibration Accuracy When using a Flash Simulator", *Conference Record of the IEEE 4th WCPEC*.
[21] G. Friesen and H.A. Ossenbrink 1997, "Capacitance effects in high-efficiency cells", *Solar Energy Materials and Solar cells* 48, 77-83.
[22] T. Roth et al. 2011, "In-depth analysis of transient errors of inline IV measurements", *Energy Procedia* 8, 82-87.

[23] J. Abe et al. 2014, "Accurate and Rapid Measurement of High-Capacitance PV Cells and Modules using Dark Current Characteristics", *Proc. of 29th EU PVSEC*.
[24] K. Ramspeck *et al.* 2014, "Accurate Efficiency Measurements on Very High Efficiency Silicon Solar Cells Using Pulsed Light Sources", *Proc. of 29th EU PVSEC*.
[25] A. Virtuani et al. 2012, "Fast and accurate methods for the performance testing of highly-efficient c-Si Photovoltaic modules using a 10 ms single-pulse solar simulator and customized voltage profiles", *Meas. Sci. Technol*. 23, 115604.
[26] B. Paviet-Salomon et al. 2016, "Accurate Determination of Photovoltaic Cell and Module Peak Power from Their Current-Voltage Characteristics", *IEEE JPV* 6(6), 1564-1575.
[27], R.Sinton, R. Pauley 2005, "Measurement of current-voltage characteristic curves of solar cells and solar modules", *Patent US7309850B2*.
[28] K. A. Emery and C. R. Osterwald 1990, "PV performance measurement algorithms, procedure and equipment," *Proc. 21st IEEE Photovoltaic Spec. Conf.,* 1068–1073.
[29] R. Gottschalg et al. 1999, "The influence of the measurement environment on the accuracy of the extraction of the physical parameters of solar cells," *Meas. Sci. Technol.,* vol. 10, no. 9, 796–804
[30] H. Qasem et al. 2011, "Analysis of key performance parameter extraction from current voltage measurements of photovoltaic devices " *Proc. 37th IEEE Photovoltaic Spec. Conf.,* 002283–002288
[31] Standard Test Method for Electrical Performance of Photovoltaic Cells Using Reference Cells Under Simulated Sunlight, ASTM Int. Std. E948-09, 2009
[32] B. Paviet-Salomon *et al.* 2017, "New guidelines for a more accurate extraction of solar cells and modules key data from their current-voltage curves", *Progress in Photovoltaics: Research and Applications* 25, 623-635.

**Acknowledgements**
This project has received funding from the Swiss KTI program within the COMET project and from the European Union's Horizon 2020 Research and Innovation programme under grant agreement No. 745601

**About the authors**

Jacques Levrat received his master of physics from EPFL, Switzerland, in 2008, with a specialization in optics and semiconductor physics. He received his Ph.D. degree from EPFL, where he was involved in the development of novel coherent light sources based on III-nitride microstructures. In 2013, he joined the CSEM PV-Center where he is in charge of metrological developments for c-Si solar cells and modules.

Jonas Geissbühler received his Ph.D. in 2015 from EPFL, Switzerland, with a thesis topic of high-efficiency silicon heterojunction solar cells. He joined the CSEM PV-Center in 2016, where his research interests include the metallization of silicon heterojunction solar cells, inkjet printing and high-efficiency silicon heterojunction solar cells.

Bertrand Paviet-Salomon received his Ph.D. degree in 2012 while he was with INES, developing laser processes for crystalline silicon solar cells. From 2012 to 2014, he was a postdoctoral researcher at the PV-Lab, EPFL. In 2014, he joined the CSEM PV-Center. His research interests include the development of high-efficiency crystalline silicon solar cells.

Matthieu Despeisse received his Ph.D. in 2006 for his work on advanced detectors at CERN in Geneva , Switzerland. He then joined EPFL in 2009 as head of the thin-film silicon photovoltaic s research team. Since 2013 he has led research activities at CSEM concerning crystalline silicon photovoltaics and metallization, with a special focus on silicon heterojunction technology, passivating contacts, silicon-based multi-junction cells, metallization and interconnection.

Christophe Ballif received his Ph.D. from EPFL, Switzerland, in 1998. In 2004 he became a full professor with the Institute of Microengineering at the University of Neuchâtel, where he directs the Photovoltaics and Thin-Film Electronics Laboratory, which is now part of EPFL. Since 2013 he has also been the director of the CSEM PV-Center. His research interests include materials for PV, high-efficiency c-Si solar cells, module technology, BIPV and energy systems.

**Enquiries**

Jacques Levrat
CSEM
Jaquet-Droz 1
Neuchâtel
Switzerland

Tel: +41 32 720 5699
Email: jacques.levrat@csem.ch
www.csem.ch